

Full Length Research Paper

Photothermal conversion in a solar collector with tilted walls

Mamadou Saliou Diallo¹, Joseph Sarr^{1*}, Mamadou Lamine Sow¹, Cheikh Mbow¹, Bassirou Ba², Ababacar Thiam³, Mactar Sall⁴ and Mamadou Mansour Kane⁵

¹Groupe de Recherches sur les Transferts (GRT), Faculté des Sciences et Techniques de l'Université Cheikh Anta Diop de Dakar, B. P. 5005 Dakar Fann, Sénégal.

²Laboratoire des Semi-Conducteurs et d'Energie Solaire, Faculté des Sciences et Techniques de l'Université Cheikh Anta Diop de Dakar, B. P. 5005 Dakar Fann, Sénégal.

³Laboratoire d'Energétique Appliquée, Ecole Supérieure Polytechnique de l'Université Cheikh Anta Diop de Dakar, B. P. 5085, Dakar, Sénégal.

⁴Centre d'Etudes et de Recherches sur les Energies Renouvelables de l'Université Cheikh Anta Diop de Dakar, B. P. 476 Dakar RP, Sénégal.

⁵Faculté des Sciences et Technologies de l'Université Amadou Hampaté Ba, B. P. 12015, Dakar, Sénégal.

Accepted 14 October, 2009

This paper presents a performance analysis of a solar air collector with tilted side faces. The northern side wall is tilted at an angle of 38° and other walls are tilted at an angle of 9° relative to the vertical. All these walls are covered with a thin reflective aluminium film. The device may be used as drier, sterilizer or cooker in rural areas. The prototype collector was designed and produced in the Study and Research Center on Renewable Energies of Cheikh Anta Diop University of Dakar. A theoretical study of heat transfer allows us to formulate the partial differential equations that govern the operation of the collector. These equations were solved numerically using a finite differences method. The agreement between the computed and experimental results for the daily global solar energy and the temperature inside the collector validate the theoretical model. The discrepancy between theory and experiment is less than 2% for the global solar radiation and there is also satisfactory agreement for the absorber temperature.

Key words: Solar collector improvement, global solar radiation, numerical modeling, heating system.

INTRODUCTION

The limited reserve of fossil fuels and the unforeseeable variations in oil prices are presently a serious issue for developing countries that do not produce hydrocarbons. Their fragile economies are easily shaken as a result of their need for fuels, leaving them with little alternative to intensively exploiting wood resources to meet basic needs, such as cooking or the sterilization of the medical instruments. This accelerates deforestation and endangers biodiversity. This article reports the results of an ex-

perimental and theoretical study of a solar collector with double glazing that uses solar energy to produce heat. When used appropriately, these collectors can contribute to tackling the energy deficit in rural areas and thus reducing the dependence of rural consumers on fossil fuels.

Many researchers have contributed to the design of the "hot box" for use as a solar cooker. El-Sebaili et al. (1994) have designed and constructed a box-type solar cooker with multi-step inner reflectors. The inner reflectors were arranged in a three-step fashion at different inclinations. A mathematical model, based on the consideration of energy balance in the different components of the device, was developed. A hot-box solar cooker was tested by Nahar et al. (1994) in an indoor solar simulator, making use of 40 and 100 mm thick transparent insulation mate-

Corresponding author. E-mail: josarr@gmail.com. Tel: +221 77 442 54 28. Fax: + 33 821 169 783.

Abbreviation: CERER - UCAD: Study and Research Center on Renewable Energies of Cheikh Anta Diop University of Dakar.

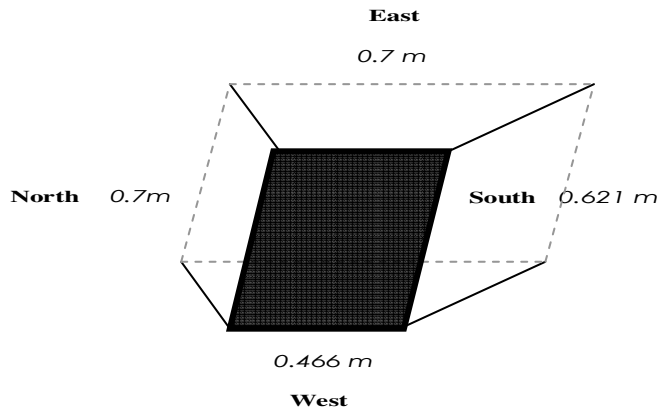


Figure 1. Interior vat.

rial, at Jodhpur, India. A simple, efficient solar cooker was designed and its performance in the Egyptian climate was evaluated by Ibrahim et al. (1995). The cooker is of the hot-box type with a plane booster mirror reflector. A program to develop, test and evaluate a solar cooker was carried out by Malik et al. (1996) with the primary objective of assessing its suitability as an alternative means of cooking using sun rays. A novel solar cooker that does not require any tracking, has been designed, fabricated and tested by Nahar (1998) and its performance has been compared with that of the hot-box solar cooker. A laboratory model of a box-type solar cooker employing a non-tracking concentrator has been designed and fabricated by Negi et al. (2005) and its thermal performance has been investigated experimentally. The concentrator, consisting of two planar reflectors positioned along an east-west axis on an inclined framework, is mounted on the box of the cooker to reflect incident solar radiation onto the base absorber of the cooker. The angle of inclination is equal to the latitude of the geographical location and is adjusted seasonally to maximize the efficiency of the device. Murty et al. (2007) developed various types of solar cookers, of both the box type and the concentrator type. A cooker with a parabolic concentrator can achieve temperatures up to nearly 250°C, making it suitable for a wide range of applications like baking, roasting and distillation, but one drawback is the intense glare produced. Harmim et al. (2008) compared the efficiency, in the Algerian Sahara, of a box-type solar cooker on two different cooking vessels of identical shape and volume, one of which had fins on its external lateral surface. The development and the popularization of cookers and solar sterilizers in rural areas are essential in the Sahel countries. In this field, the research team of CERER-UCAD (Study and Research Center on Renewable Energies of Cheikh Anta Diop University of Dakar) produced a prototype double-glazed solar collector (Sarr J., Development of a solar sterilizer, internal report, 1985). The bottom of the collector is a metal plate painted black. The side faces are tilted and covered with a thin

reflective aluminium film to allow a better collection of the solar radiation and its concentration on the black metal plate. The global solar radiation and the absorber plate temperature are measured and simulations done using specially developed software are then compared with the experimental data (Diallo, 2009).

DESCRIPTION OF THE COLLECTOR AND MEASURING DEVICES

The collector is constructed mainly from plywood wood plates, a blackened sheet and transparent covers and has the following main components: the box, the interior vat, the lid of the box and insulation.

The box is a cube made from laminated wood of 19 mm thickness.

The interior vat, built with laminated wood of 15 mm thickness, is a truncated and inverted pyramid (Figure 1). The side faces are covered with a thin aluminium film that reflects the incident solar rays towards a sheet painted in black that rests at the bottom of the vat (absorber plate). The total volume of the vat is approximately 0.1 m³.

The lid consists of two transparent covers: the external one is made of 3 mm-thick Plexiglas and the internal cover of 4 mm-thick clear glass. The space between these two covers equals 15 mm. This setup makes the system resistant to external shocks and to the relatively high internal temperatures inside the collector.

Insulation is provided by the space between the interior vat and the external box. This space occupies a volume of 0.16 m³ and is filled with glass wool.

The collector was initially tested in the same manner as a sterilizer in the public dispensary of the village of Malicounda (Department of Mbour in Senegal). The follow-up of the installation under real operating conditions was the subject of many scientific and technical expeditions.

Measurements were carried out by the Department of the CERER-UCAD in charge of the scientific and technical follow-up with the following equipment: 1) 1 thermocouple digital thermometer which can display 6 temperature measurements simultaneously (model THERMODIG N 1300). 2) 2 thermometers (alcohol and mercury) fixed permanently on the southern wall of the interior vat. 3) 1 LCD solarimeter (HAENNI Solar SN/8623 model) measuring the global solar power (W m⁻²) and calculating the accumulated energy in Wh m⁻².

The measured parameters are: the absorber temperature (black plate), the temperature inside the interior vat, the outside temperature and the global solar power.

STUDY OF HEAT TRANSFER INSIDE THE COLLECTOR

Simplifying assumptions

1) Heat transfer through the reflective side walls is neglected. 2) Multiple reflections between the two transparent covers are neglected. 3) The air inside the collector is transparent. 4) All the components of the collector are initially at the same temperature as the ambient air.

Modes of heat transfer inside the box (Figure 2)

η ($=38^\circ$) is the inclination angle, relative to the vertical, of the Southern reflective wall. θ ($=9^\circ$) is the inclination angle of the other side reflective walls.

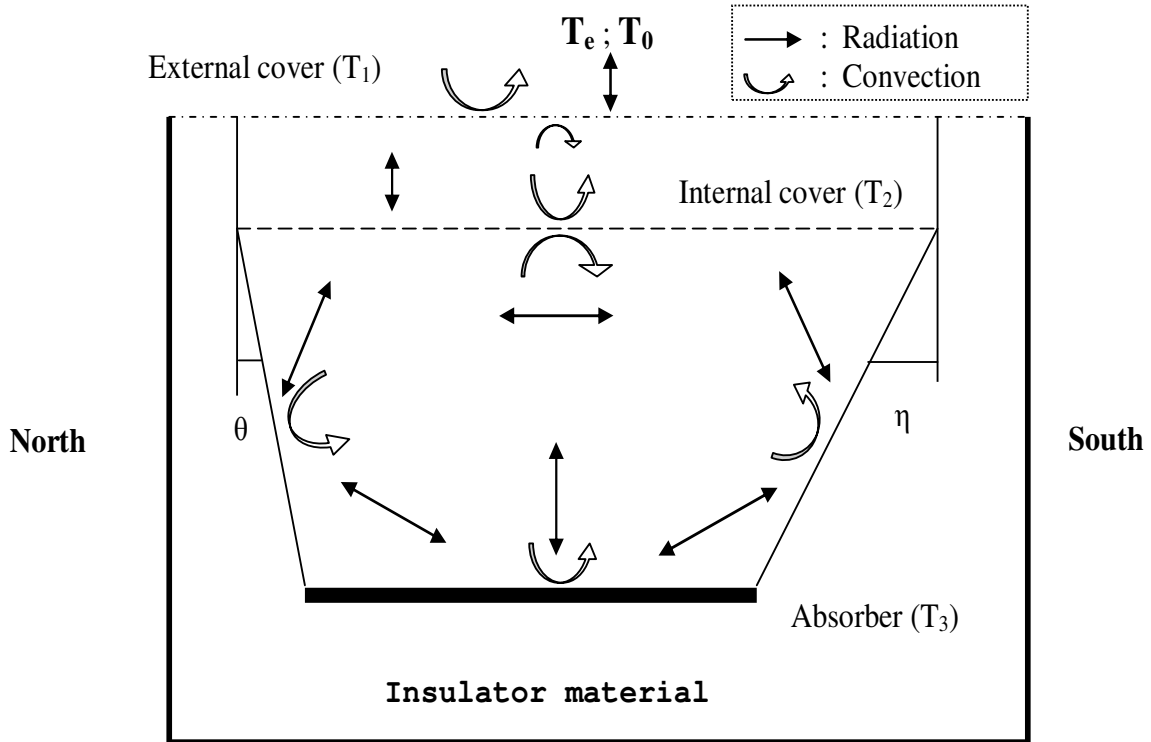


Figure 2. Modes of heat transfer in the device.

Calculation of the radiation components

Direct solar radiation

This is the radiation going through the atmosphere without undergoing modifications. It can be calculated by the following empirical formula reported by Guèye (1997), Thiam (1998, 2008):

$$S^* = \phi \exp(M \xi) \sin(H) \tag{1}$$

Where; ϕ is the incident solar flux on a plane normal to the solar rays and is defined by:

$$\phi = C (1 + 0.034 \cos [0.986 (j-3)]) \tag{2}$$

Where; $C = 1367 \text{ Wm}^{-2}$

Diffuse solar radiation

This is the proportion of solar radiation scattered by solid particles or liquid droplets in the atmosphere, denoted D^* . It is expressed by the following correlations reported by Thiam (2008):

$$\text{Polluted sky: } D^* = 164[\sin(H)]^{0.4} \tag{3}$$

$$\text{Clear sky: } D^* = 125[\sin(H)]^{0.4} \tag{4}$$

$$\text{Very clear sky: } D^* = 87[\sin(H)]^{0.4} \tag{5}$$

$$\text{Milky sky: } D^* = 187[\sin(H)]^{0.4} \tag{6}$$

Global radiation

The global radiation G^* is the sum of the direct and scattered radiations.

$$G^* = \phi \exp[M\xi] \sin(H) + D^* \tag{7}$$

The temperature distribution (Sall, 1982; Sène, 2003)

Heat balance on the external cover is expressed as;

$$\frac{\partial T_1}{\partial t} = \frac{\alpha_1 \Phi_{r,i} \rho_1}{e_1 C_{p1}} + \Phi_{r,2-1} + \Phi_{c,2-1} - \Phi_{r,0-1} - \Phi_{c,e-1} \tag{8}$$

On the internal cover, it is expressed as

$$\frac{\partial T_2}{\partial t} = \tau_1 \frac{\alpha_2 \Phi_{r,i}}{\rho_2 e_2 C_{p2}} + \frac{4 R_{al} \tau_1 \tau_2 \alpha_3 \Phi_{r,i}}{\rho_2 e_2 C_{p2}} + \Phi_{r,3-2} + \Phi_{c,3-2} + \Phi_{r,2-1} + \Phi_{c,2-1}, \tag{9}$$

and on the absorber plate as

$$\frac{\partial T_3}{\partial t} = \frac{\tau_1 \tau_2 \alpha_3 \Phi_{r,i}}{\rho_3 e_3 C_{p3}} + \frac{4 R_{al} \tau_1 \tau_2 \alpha_3 \Phi_{r,i}}{\rho_3 e_3 C_{p3}} + \Phi_{r,3-2} + \Phi_{c,3-2}. \tag{10}$$

NUMERICAL SOLUTION

The three first-order equations 8, 9 and 10 govern the behavior of the operating collector and are solved by the method of finite differences.

Time discretization yields the following system:

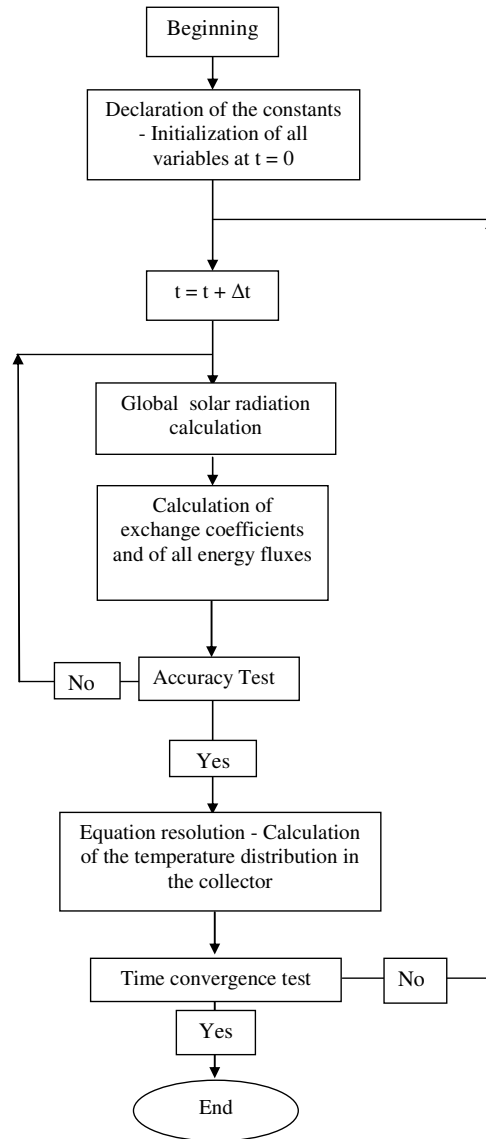


Figure 3. Algorithm calculation.

$$\begin{aligned}
 T_1^{n+1} &= \left[1 - \frac{\Delta t}{\rho_1 e_1 C p_1} (h_{c,e-1} + h_{c,2-1} + h_{r,1-0} + h_{r,2-1}) \right] \times T_1^n + \frac{\Delta t (h_{c,2-1} + h_{r,2-1})}{\rho_1 e_1 C p_1} \times T_2^n \\
 &+ \frac{\Delta t}{\rho_1 e_1 C p_1} [\alpha_1 \Phi_{r,1} + h_{c,e-1} T_a + h_{r,1-0} T_0] \\
 T_2^{n+1} &= \left[1 - \frac{\Delta t}{\rho_2 e_2 C p_2} (h_{c,3-2} + h_{c,2-1} + h_{r,3-2} + h_{r,2-1}) \right] \times T_2^n + \frac{\Delta t (h_{c,3-2} + h_{r,3-2})}{\rho_2 e_2 C p_2} \times T_3^n \\
 &+ \frac{\Delta t (h_{c,2-1} + h_{r,2-1})}{\rho_2 e_2 C p_2} \times T_1^n + \frac{\Delta t \tau_1 \alpha_2}{\rho_2 e_2 C p_2} [1 + 4R_{a1} \tau_2] \times \Phi_{r,i} \\
 T_3^{n+1} &= \left[1 - \frac{\Delta t}{\rho_3 e_3 C p_3} (h_{c,3-2} + h_{r,3-2}) \right] \times T_3^n + \frac{\Delta t (h_{c,3-2} + h_{r,3-2})}{\rho_2 e_2 C p_2} \times T_2^n \\
 &+ \frac{\Delta t \tau_1 \tau_2 \alpha_3}{\rho_3 e_3 C p_3} [1 + 4R_{a1} \tau_2] \times \Phi_{r,i}
 \end{aligned} \tag{11}$$

The system is then written in the following matrix form:

$$[T^{n+1}] = [MATRIX] \times [T^n] + [B^n] \tag{12}$$

Where T^n is the temperature at time point n . This system enables us to predict the temperature change between time points n and $n+1$, over a time step of Δt . The calculation relies on the temperature distribution inside the collector being constant over time.

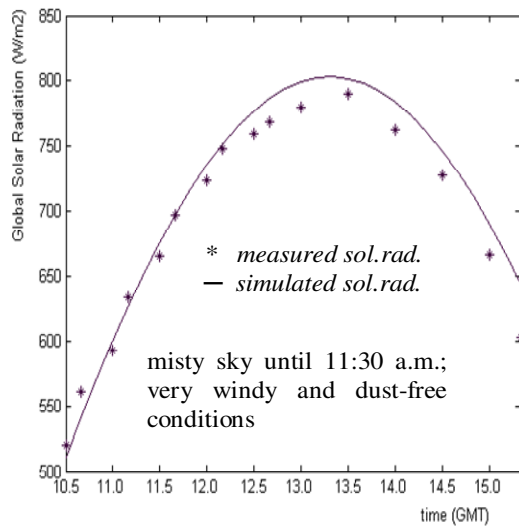
The simulation algorithm is shown in Figure 3 and was implemented using MatLab 6.5, a high-performance software for technical computing that combines computation, visualization and programming in an interactive user-friendly environment.

RESULTS AND DISCUSSION

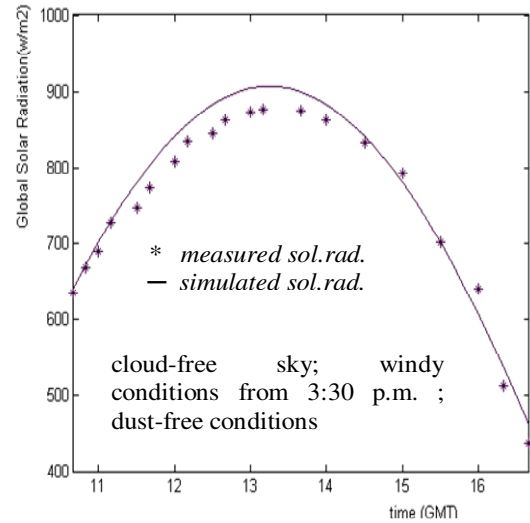
Global solar radiation

Solar fluxes measured over several days are plotted as shown in Figure 4. The graphs reach a maximum around 13:00 GMT and decay on either side.

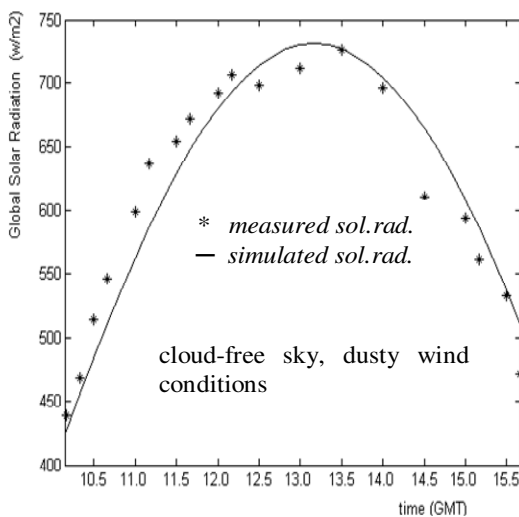
There is satisfactory agreement between the simulated



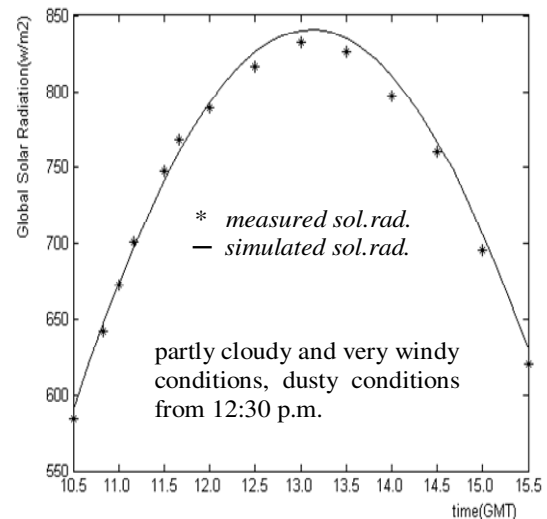
a) March, 15



b) March, 26



c) April, 11



d) April, 24

Figure 4. Simulated and experimental variation of the solar flux on different days.

and experimental curves, considering slight variations due to fog, clouds or dust in the atmosphere. The calculated global solar radiation values are slightly higher (2% higher than the maximum), but, by and large, the software has shown to be adequate for the design of the solar device.

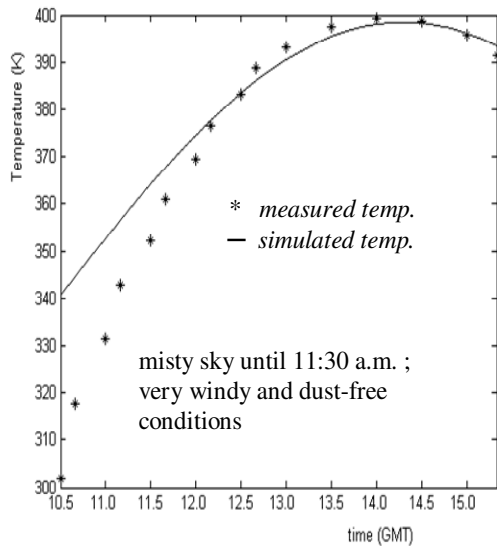
Temperature distribution

The time step for the numerical integration was set to $\Delta t = 100$ s. Reducing Δt by 5% increases the calculation time by 20% but had negligible effect on the maximum value

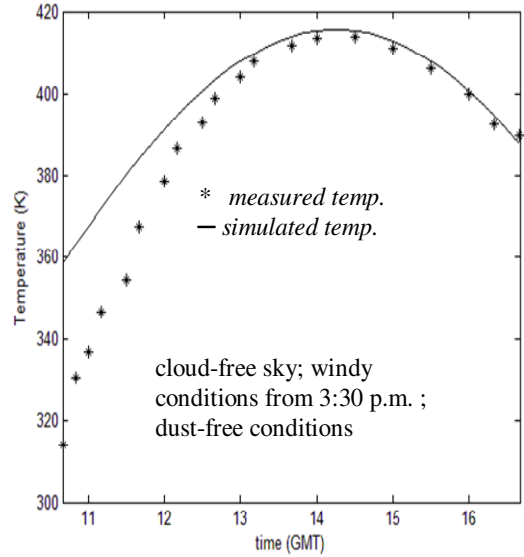
of the absorber plate temperature.

Figure 5 shows the variation of the absorber plate temperature (T_3) with time on different days. The shape of the curves is similar for each day and follows the evolution of global solar radiation, albeit with a short time delay due to the time to heat and cool the absorber plate. The temperature reaching its maximum around 14:00 GMT, then falls rather abruptly as the sun starts to set.

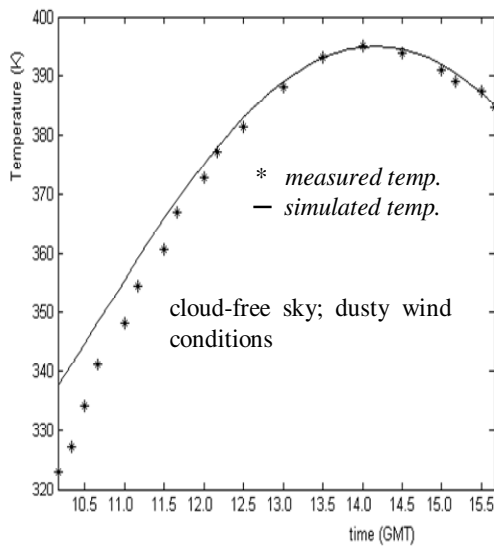
The theoretical and experimental data are in satisfactory agreement around midday and during the afternoon. There is more discrepancy in the mornings, however, mainly as a result of the time delay in heating the collec-



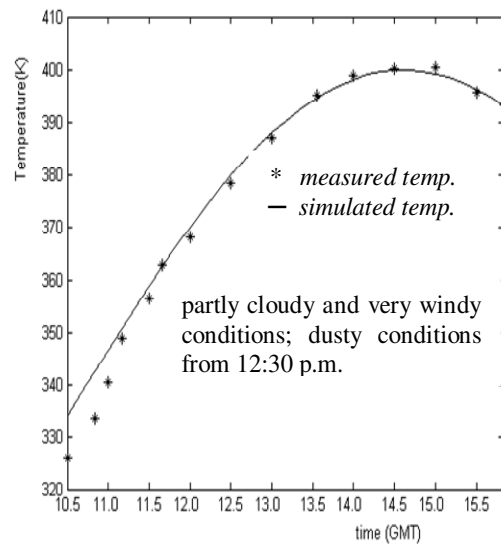
a) March, 15



b) March, 26



c) April, 11



d) April, 24

Figure 5. Simulated and experimental variation of the absorber plate temperature on different days.

tor and of heat loss through the non ideal insulated walls.

Conclusion

This work has described a photothermal conversion device exposed to solar radiations. This “hot box” device has versatile uses such as cooking, drying food and

agriculture products and the sterilization of medical instruments.

A thorough analysis of the various modes of heat transfer inside the collector made it possible to highlight the significant modes of heat transfer between the cover, the absorber plate and the ambient environment.

The temperature change of the various components of the collector was recorded every half-hour.

Owing to the complexity of the partial differential equa-

tions for the temperature of the various components, they were solved numerically using the MatLab 6.5 software. The numerical model made it possible to determine the time course of the temperature of the various elements on different days. The values of the solar radiation were also calculated. There is reasonably good agreement between theory and experiment, considering the approximate knowledge of certain astronomical or atmospheric parameters and the thermal exchange coefficients that are generally based on empirical relations.

Appendixes

Solar flux absorbed by the external cover, $\Phi_{r,1-i} = \alpha_1 S \Phi_{r,i}$ (A1)

Solar flux absorbed by the internal cover, $\Phi_{r,2-i} = \tau_1 \alpha_2 S \Phi_{r,i}$ (A2)

Solar flux absorbed by the absorber plate, $\Phi_{r,3-i} = \tau_1 \tau_2 \alpha_3 S \Phi_{r,i}$ (A3)

Energy flux radiated by the external cover towards the sky (Pierson, 1986),

$\Phi_{r,1-0} = h_{r,1-0} S (T_0 - T_1)$ with $h_{r,1-0} = 4\epsilon_1 \sigma_1 (T_0)^3$ if $T_1 - T_0 < 100K$ (A4)

Thermal flux exchanged by convection between the external cover and the outside ambient air,

$\Phi_{c,1-e} = h_{c,1-e} S (T_e - T_1)$ with $h_{c,1-e} = 5.67 + 3.86V$ (A5)

from Woertz et Hottel cited by Sall (1982).

Thermal flux exchanged by convection between the two covers (Barka, 1997).

$\Phi_{c,2-1} = h_{c,2-1} S (T_2 - T_1)$ with $h_{c,2-1} = \frac{k_{f,2-1} N}{e_{f,2-1}}$ (A6)

Energy flux exchanged by radiation between the two covers

$\Phi_{r,2-1} = h_{r,2-1} S (T_2 - T_1)$ with $h_{r,2-1} = \sigma (T_1^2 + T_2^2) (T_1 + T_2)$ (A7)

Energy flux exchanged by radiation between the internal cover and the absorber

$\Phi_{r,3-2} = h_{r,3-2} S (T_3 - T_2)$ with $h_{r,3-2} =$

$h_{r,3-2} = \frac{\sigma (T_3^2 + T_2^2) (T_3 + T_2)}{(1/\epsilon_3 + 1/\epsilon_2 - 1)}$ (A8)

from Combes cited by Sall (1982).

Thermal flux due to the convection exchange between the internal cover and the absorber (Barka, 1997).

$$\Phi_{c,3-2} = h_{c,3-2} S (T_3 - T_2) \text{ with } h_{c,3-2} = \frac{h_{c,3-2} \text{Nu}_{3,2}}{e_{f,3-2}} \quad (\text{A9})$$

Nomenclature

Symbols

C	solar constant, Wm^{-2}
C_p	specific heat, $Wkg^{-1}K^{-1}$
D^*	diffuse solar radiation, Wm^{-2}
e	thickness, m
G	gravitational field, ms^{-2}
G^*	global solar radiation, Wm^{-2}
H	angular height, °
h	heat transfer coefficient, $Wm^{-2}K^{-1}$
j	year day number
k	thermal conductivity coefficient, $Wm^{-1}K^{-1}$
M	atmospheric mass number
n	time index superscript
R	reflection coefficient
S	area, m^2
S^*	direct solar radiation, Wm^{-2}
T	temperature, K
t	time, s
V	wind speed, ms^{-1}
α	absorption coefficient
Δt	time step, s
ϵ	emissivity
η, θ	inclination angles of reflective walls, °
ξ	optic density
ρ	density, $kg m^{-3}$
σ	Stefan-Boltzmann constant, $Wm^{-2}K^{-4}$
τ	transmission coefficient
Φ	energy flux, W
ϕ	incident solar flux on a plan normal to the solar rays, W

Subscripts

0	sky
1	external cover
2	internal cover
3	absorber plate
al	aluminium
c	convection
e	external ambient conditions
f	fluid
i	incident solar rays
r	radiation

REFERENCES

- Barka M (1997). Couplage d'un distillateur sphérique à balayage avec un capteur plan solaire : Etude théorique et expérimentale. Thèse de

- Doctorat, Spécialité Energétique, Université Claude Bernard, Lyon, France.
- Diallo MS (2009). Etude de la conversion photothermique dans une enceinte isolée. Thèse de doctorat en énergie solaire (en préparation), Département de Physique, Faculté des Sciences et Techniques, Université Cheikh Anta Diop, Dakar, Sénégal.
- El-Sebaï AA, Domanski R, Jaworski M (1994). Experimental and theoretical investigation of a box-type solar cooker with multi-step inner reflectors. *Energy* 19(10) : 1011-1021.
- Guèye K (1997). Modélisation analytique et numérique du champ thermique dans une dalle récupératrice destinée à la production d'eau chaude sanitaire. Thèse de Docteur-Ingénieur- Ecole Supérieure polytechnique, Université Cheikh Anta Diop, Dakar, Sénégal.
- Harmim A, Boukar M, Amar M (2008). Experimental study of a double exposure solar cooker with finned cooking vessel. *Solar Energy*, 82(4): 287-289.
- Ibrahim SMA, El-Reidy MK (1995). The performance of a solar cooker in Egypt. *Renewable Energy* 6(8): 1041-1050.
- Malik AQ, Hussien HB (1996). Development of a solar cooker in Brunei Darussalam. *Renewable Energy* 7(4) 419-425.
- Murty VVS, Gupta A, Mandloi N, Shukla A (2007). Evaluation of thermal performance of heat exchanger unit for parabolic solar cooker for off-place cooking. *Indian J. Pure Appl. Phys.* 45(9): 745-748.
- Nahar NM (1998). Design, development and testing of a novel non-tracking solar cooker. *Int. J. Energy Res.* 22(13): 1191-1198.
- Nahar NM, Marshall RH, Brinkworth BJ (1994). Studies on a hot box solar cooker with transparent insulation materials. *Energy Conversion Manage.* 35(9): 787-791.
- Negi BS, Purohit I (2005). Experimental investigation of a box-type solar cooker employing a non-tracking concentrator. *Energy Conversion Manage.* 46(4): 577-604.
- Pierson P (1986). Etude théorique et expérimentale de systèmes thermiques en régime instationnaire : Echangeurs, capteurs solaires et installations solaires actives. Thèse de Doctorat ès Sciences. Université de Reims - Champagne - Ardenne UFR Sciences Exactes et Naturelles, France.
- Sall M (1982) Caractérisation théorique et expérimentale d'un insolateur plan à air. Thèse de Doctorat de Spécialité en thermodynamique et énergétique, Université de Perpignan, France.
- Sène M (2003). Dimensionnement d'un capteur solaire à air d'un système ouvert de climatisation par évaporation. Mémoire de DEA - Ecole Supérieure Polytechnique, Dakar, Sénégal.
- Thiam A (1998). Stockage de la chaleur dans un capteur matériau fusible. Mémoire de DEA- Ecole Supérieure Polytechnique, Dakar, Sénégal.
- Thiam A (2008). Stockage et récupération de la chaleur dans un capteur à changement de phase : Application à un Chauffe-Eau Solaire. Thèse de Doctorat de troisième cycle en physique- Ecole Supérieure Polytechnique, Université Cheikh Anta Diop, Dakar, Sénégal.